REPORT DOCUMENTATION PAGE

AFRL-SR-AR-TR-09-0218

PLEASE DO NOT RETURN YOUR FORM TO THE ABOVE ADDRESS.

1. REPORT DATE *(DD-MM-YYYY)*	2. REPORT TYPE	3. DATES COVERED (From – To)
	Final Technical Report	1 APRIL 2007 – 30 NOVEMBER 2007

4. TITLE AND SUBTITLE
RARE EARTH ALUMINOPHOSPHOSILICATE GLASS PRECURSORS FOR CERAMIC-MATRIX-COMPOSITES (REAPS CMC'S)

5a. CONTRACT NUMBER

5b. GRANT NUMBER
FA9550-07-1-0371DEF

5c. PROGRAM ELEMENT NUMBER

6. AUTHOR(S)
DR. WILLIAM T. PETUSKEY

5d. PROJECT NUMBER

5e. TASK NUMBER

5f. WORK UNIT NUMBER

7. PERFORMING ORGANIZATION NAME(S) AND ADDRESS(ES)
BOX 871604
TEMPE, AZ 85287-1604

8. PERFORMING ORGANIZATION REPORT NUMBER

9. SPONSORING/MONITORING AGENCY NAME(S) AND ADDRESS(ES)
USAF/AFRL
AFOSR
875 North Randolph Street
Arlington VA 22203

10. SPONSOR/MONITOR'S ACRONYM(S)
AFOSR

11. SPONSORING/MONITORING AGENCY REPORT NUMBER
N/A

12. DISTRIBUTION AVAILABILITY STATEMENT

Distribution Statement A: Approved for public release. Distribution is unlimited.

13. SUPPLEMENTARY NOTES

14. ABSTRACT

This project was dedicated to assessing the utility of rare earth aluminophosphosilicate (REAPS) glasses within the Al2O3-AlPO4-LaPO4-SiO2 system as precursors for fabricating ceramic-matrixcomposites of mullite (Al6Si2O13) and monazite (LaPO4). The specific objective was to investigate selected issues for devising strategies of low-temperature pathways of viscous sintering of glass powders and crystallization anneals to produce dense monolithic ceramics of very fine textures. The ultimate goal, beyond the scope of this work, will eventually lead to innovating low temperature synthesis routes for ceramic composites of high fracture toughness and high temperature applications.

15. SUBJECT TERMS

16. SECURITY CLASSIFICATION OF:			17. LIMITATION OF ABSTRACT	18. NUMBER OF PAGES	19a. NAME OF RESPONSIBLE PERSON
a. REPORT	b. ABSTRACT	c. THIS PAGE	Unclassified	21	19b. TELEPONE NUMBER (*Include area code*)
Unclassified	Unclassified	Unclassified			(703)

AIR FORCE OFFICE OF SCIENTIFIC RESEARCH

DTIC Data

Purchase Request Number:	FQ8671-0700696
BPN:	F1ATA06334B012
Proposal Number:	06-NA-243
Research Title:	RARE EARTH ALUMINOPHOSPHOSILICATE GLASS PRECURSORS FOR CERAMIC-MATRIX-COMPOSITES (REAPS CMC'S)
Type Submission:	~~New Work Effort~~ Final Report
Inst. Control Number:	FA9550-07-1-0371DEF
Institution:	ARIZONA STATE UNIVERSITY
Primary Investigator:	Dr. William T. Petuskey
Invention Ind:	none
Project/Task:	2306B / X
Program Manager:	Dr. Joan Fuller

Objective:

This project will investigate the use of high temperature liquids and glasses of aluminate-phosphate chemistry as synthetic pathways for producing ceramic matrix composites of highly functional microstructures and nanostructures. The target materials are contained within the family of alumina-rare earth monazites (Al2O3-LaPO4 and Al2O3-YPO4). The ultimate goal will be a deep understanding of the solidification and crystallization processes that will enable the design and fabricate microstructures.

Approach:

Most applications of ceramics rely as much on the properties induced by their microstructures as on the intrinsic properties of the individual phases. Therefore it is important to develop a fundamental understanding of the crystallization and glass formation of the ceramic oxide phosphate systems proposed in this project. The kinetics of crystallization will be studied via NMR, x-ray diffraction, calorimetry, electron microprobe and optical methods. The project will also evaluate the liquidus surfaces and subsolidus compatibility relationships of the high temperature phase diagrams. Thermochemical models of the liquids and glasses will be developed that will relate to the driving forces of crystallization. The goal will be to develop practical theoretical models that will enable the design of ceramic composites of functional microstructues.

Progress:

Year: 2008 **Month:** 07 **Final**

This project was dedicated to assessing the utility of rare earth aluminophosphosilicate (REAPS) glasses within the Al2O3-AlPO4-LaPO4-SiO2 system as precursors for fabricating ceramic-matrixcomposites of mullite (Al6Si2O13) and monazite (LaPO4). The specific objective was to investigate selected issues for devising strategies of low-temperature pathways of viscous sintering of glass powders and crystallization anneals to produce dense monolithic ceramics of very fine textures. The ultimate goal, beyond the scope of this work, will eventually lead to innovating low temperature synthesis routes for ceramic composites of high fracture toughness and high temperature applications.

In essence, this was a seed project that, over the course of six months, had the functional objective of providing sufficient proof of concept to justify proposing longer-range investigations. As such, we have been nurturing a collaboration aimed at forming a broad-based, multi-PI project. If, and when, funded, this effort will involve several investigators, research groups and funding from both countries. This work will carry out highly integrated experimental and theoretical studies so as to understand the early events of nucleation and growth in REAPS glasses. This information is essential for optimizing fabrication protocols of ceramic-matrixnano-

Progress:

Year: 2008 **Month:** 07 **Final**

composites.
The current project reported here followed earlier, exploratory research on the fundamental physical and chemical properties of REAPS glasses (conducted under AFOSR grant FA9550-004-1-0153). In that project, compositional trends of glass transition and crystallization temperatures were evaluated so that the best compositions could be identified to balance the competing requirements of viscous sintering and crystallization. At the same time, a primitive model of the structural chemistry of the glass was developed, which also fed into our longerrange objectives.
For this project, the following studies were undertaken:
1. Viscosity and viscous sintering studies were carried on glass samples of composition 40-60 mol% Al6Si2O13 and 60-40 mol %LaPO4. This corresponds to crystalline composites of about 80 vol% mullite and 20 vol% monazite once the glass system was fully crystallized. The viscosities of were experimentally determined as a function of temperature by applying the Frenkel and Scherer interpretations of sintering studies. These were compared to the viscosities inferred from the glass transition temperature and temperature range measured by differential scanning calorimetry (DSC). There was very good agreement, especially considering that REAPS glasses are known to be very structurally ¿fragile¿ in vernacular language of glass and glass theory. This work demonstrated that reliable predictions can be made on the densification of glass powders using information obtained by thermal analysis.
2. Sol gel chemical techniques were explored as a means to produce xerogel glasses that were similar to the thermal properties of thermal glasses produced by quenching high temperature melts. While somewhat different in their crystallization behavior, this study provided encouraging results indicating that they can be used for large volume synthesis of glasses as low temperature precursors for high temperature ceramic composites.
3. One unexpected, but intriguing, result was the discovery of a synthetic pathway of making very low density foams (10-12% of theoretical density) based upon mullite-monazite composite ceramics. This suggests an ability to make mechanically toughened ceramic foams.

Final Report

Rare Earth Aluminophosphosilicate Glass Precursors for Ceramic-Matrix-Composites (REAPS CMC's)

A research project sponsored by the
Air Force Office of Sponsored Research

(AFOSR Grant Award #: F9550-07-1-0371)

For the research period 4/1/07 to 11//30/07

submitted July 11, 2008

by

William T. Petuskey, Principal Investigator
Professor and Chair, Department of Chemistry & Biochemistry
Professor, School of Materials
Arizona State University
Box 871604; Tempe, AZ 85287-1604
480/965-4430; wpetuskey@asu.edu

I. Report Summary

This project was dedicated to assessing the utility of rare earth aluminophosphosilicate (REAPS) glasses within the Al_2O_3-$AlPO_4$-$LaPO_4$-SiO_2 system as precursors for fabricating ceramic-matrix-composites of mullite ($Al_6Si_2O_{13}$) and monazite ($LaPO_4$). The specific objective was to investigate selected issues for devising strategies of low-temperature pathways of viscous sintering of glass powders and crystallization anneals to produce dense monolithic ceramics of very fine textures. The ultimate goal, beyond the scope of this work, will eventually lead to innovating low temperature synthesis routes for ceramic composites of high fracture toughness and high temperature applications.

In essence, this was a seed project that, over the course of six months, had the functional objective of providing sufficient proof of concept to justify proposing longer-range investigations. As such, we have been nurturing a collaboration aimed at forming a broad-based, multi-PI project. If, and when, funded, this effort will involve several investigators, research groups and funding from both countries. This work will carry out highly integrated experimental and theoretical studies so as to understand the early events of nucleation and growth in REAPS glasses. This information is essential for optimizing fabrication protocols of ceramic-matrix-*nano*-composites.

The current project reported here followed earlier, exploratory research on the fundamental physical and chemical properties of REAPS glasses (conducted under AFOSR grant FA9550-004-1-0153). In that project, compositional trends of glass transition and crystallization temperatures were evaluated so that the best compositions could be identified to balance the competing requirements of viscous sintering and crystallization. At the same time, a primitive model of the structural chemistry of the glass was developed, which also fed into our longer-range objectives.

For this project, the following studies were undertaken:

1. Viscosity and viscous sintering studies were carried on glass samples of composition 40-60 mol% $Al_6Si_2O_{13}$ and 60-40 mol %$LaPO_4$. This corresponds to crystalline composites of about 80 vol% mullite and 20 vol% monazite once the glass system was fully crystallized. The viscosities of were experimentally determined as a function of temperature by applying the Frenkel and Scherer interpretations of sintering studies. These were compared to the viscosities inferred from the glass transition temperature and temperature range measured by differential scanning calorimetry (DSC). There was very good agreement, especially considering that REAPS glasses are known to be very structurally "fragile" in vernacular language of glass and glass theory. This work demonstrated that reliable predictions can be made on the densification of glass powders using information obtained by thermal analysis.

2. Sol gel chemical techniques were explored as a means to produce xerogel glasses that were similar to the thermal properties of thermal glasses produced by quenching high temperature melts. While somewhat different in their crystallization behavior, this study provided encouraging results indicating that they can be used for large volume synthesis of glasses as low temperature precursors for high temperature ceramic composites.

3. One unexpected, but intriguing, result was the discovery of a synthetic pathway of making very low density foams (10-12% of theoretical density) based upon mullite-monazite composite ceramics. This suggests an ability to make mechanically toughened ceramic foams.

II. Summary of Project Results

There were two principal objectives for this project. One was to demonstrate that glasses can be effective precursors for forming dense ceramic composites. This project succeeded in that regard. Handling and sintering glass powders is inherently faster than relying on sintering processes of the crystalline counterparts. The reason is that in an thermodynamically unstable, but kinetically arrested state, oxide materials can exhibit faster mass transport in the viscous state than usually seen in crystalline solids at the same temperature.

In conducting our studies, we focused on developing a rapid and reliable method for estimating the viscosity of REAPS glasses as a function of temperature and composition. By measuring the viscosity directly from the sintering of glass powders, we were able to confirm that it was possible to reliably estimate the viscosity from the thermal analysis (by DSC) of the glass transition temperature. That is, measurement of the temperature and temperature range of the glass transition could be used for evaluating the viscosity-temperature relationship. Typically, the errors we observed were on the order of a factor of two, which is exceptional for a property that will vary 12 to 13 orders of magnitude for a single material.

Armed with this ability to predict viscosity, coupled with reliable models for viscous sintering of glass powders, it is now possible to carry out optimization studies as to best conditions for densifying glass powders and avoid premature crystallization. This implies, however, that viscous sintering is conducted well below crystallization temperatures. Our strategy has been to increase the chemical and structural complexity of glasses so that crystallization is forced to occur at higher temperatures. Again, we succeeded with that strategy for REAPS glasses, where we were able to extend the crystallization temperature to as much as 200°C greater than T_g. Essentially, we have focused on the most optimal compositions in the vicinity of 50 mol% $Al_6Si_2O_{13}$ and 50 mol% $LaPO_4$ which would yield a composite of 80 vol% mullite and 20 vol% monazite by solids content. This is a very attractive composition for producing composites.

The second major objective of this project was to identify a useful low temperature mechanism for producing large quantities of REAPS glasses. Synthesis using melt-quench procedures is somewhat cumbersome because of the high temperatures involved (~2000°C) and having to quench samples that are less than approximately 1 mm diameter. While such procedures can be scaled up for larger scale production, we were interested in exploring procedures that would be more amenable for laboratory production and of potential commercial interest. Again, we have had some significant measure of success.

We focused a procedure that began with a hydro-gelation chemistries that in some cases introduced organic components. With low temperature treatment, these materials were converted to xerogels that possessed many of the same properties of the thermal glasses. Often we found that the glass transition temperatures were the same as the thermal glasses of the same temperature. However, we typically found the crystallization temperatures to be lower, thereby less advantageous with respect to viscous sintering under atmospheric pressures. In the end, there were several positive and attractive features that were discovered, suggesting that these gels will be useful for making dense composites.

The most intriguing result from these studies is that we discovered conditions where low-density foams could be produced, that in the end consisted of mullite-monazite foams with high temperature, morphological stabilities. Bulk densities as low as 10 to 12 vol % solids (i.e., up to 84% open porosity, 4 vol % closed porosity) could be routinely made. When crystallized, these

structures were quite stable to above 1200°C. In fact, foams anncaled seven days at 1400°C, saw only about a 10% reduction in volume. The attractive aspect is that the cellular structurc is formed by a two-phase mullite-monazite composite, which has been our objcctive in producing high fracturc toughness ceramics. We foresee an advantage to low density, high porosity ceramics that are tough and wear resistant.

We were able to demonstrate that it was possible to produce dense, translucent glasses and glass-ceramic composites via hot pressing at relatively low temperatures (925°C). Once crystallized, these materials were stable to much higher temperatures. It is expected that this will be an attractive approach in producing ceramic-matrix-*nano*composites that have attractive mechanical properties.

Acknowledgements

The principal investigator sincerely appreciates the financial support and encouragement of the Air Force Office of Scientific Research, supplied through the Directorate of Aerospace and Materials Sciences office on Ceramics and Nonmetallic Materials program (Dr. Joan Fuller, director).

III. Technical Results

III.A. Viscosity and Sintering Studies of $Al_6Si_2O_{13}$–$LaPO_4$ glasses

Densification of glass powders by viscous sintering is generally faster than densification of crystalline powders by diffusion mechanisms presuming that a stable glass can be formed of the samc general composition. For cases like REAPS glasses, stability relies on structural complexity due to the multiple anionic structural species that form the tetrahedral network. This complexity provides an important barrier to crystal nucleation and growth since this must be preceded by compositional segregation and degradation of the glass network.

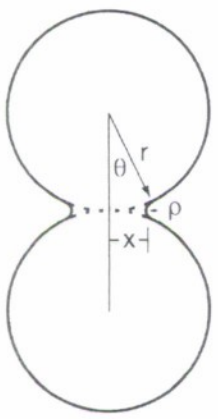

Fig. 1. Geometry of sintering neck to form between spherical glass beads. Basis of Frenkel model.

Initial structural studies have shown that the glass network is dominated by the corner linking of AlO_4 tetrahedra to SiO_4 and PO_4 tetrahedra. On the other hand, there is relatively little linking between silicon and phosphorus species because of the repulsion of their relatively high electrostatic cationic cores. In fact, the existence of AlO_6 octahedra in these glasses is almost non-existent indicating that the stabilization of four-fold coordinated aluminum is interdependent with its insertion into the glass network.

This is contrary to what is observed in crystalline solids where six-fold coordination of aluminum is most common. The process of crystal nucleation from the glass is therefore dependent on a complex series of steps that involves first compositional segregation and concurrent structural relaxation in the amorphous state. If the rate of compositional segregation is relatively slow compared to structural relaxation due to viscous flow under shear forces, then densification by viscous

sintering can be exploited without the interference of crystallization.

Compared to most sintering theories, the theory of initial-stage viscous sintering is well understood and quantitative. Based upon an initial proposal of Frenkel[2], the energy dissipated in viscous flow is equivalent to the energy released due to surface area reduction during densification, i.e., when necks form between particles. A geometrical analysis between two coalescing particles, as depicted in Fig. 1, indicates that

$$\frac{x^2}{r} = \left(\frac{3\gamma}{2\eta}\right)t \qquad (1)$$

Where x is the neck radius that has formed between two particles, r is the radius of the particles themselves, γ is surface energy, t is sintering time and η is viscosity. Whereas the rate of sintering can be examined with foreknowledge of the viscosity at a given temperature, the viscosity can conversely be determined by measuring the rate of sintering.

We carried out experimental studies on the rates of sintering of $Al_6Si_2O_{13}$–$LaPO_4$ glass beads and powders of different compositions for the purpose of measuring their viscosities. Two experimental methods were employed, both of which were compared to the viscosities inferred from glass transition behavior measured by differential scanning calorimetry. These methods were chosen since homogeneous glass powders and small beads could be readily produced for the range of desired REAPS compositions. The viscosities were extracted from either the rate of densification of powder compacts or by microscopic observations of the rate of neck formation between small glass beads.

III.A.1. *Viscosities from Neck Formation Measurements between Frenkel Beads*. The first experimental method was based upon microscopic observations of the formation and growth of the sintering neck to form between two macroscopic beads at high temperatures. The geometry is essentially that shown in Fig. 1. Figure 2 shows a sintering neck as viewed microscopically along the common axis of the two beads. The diameter, and thereby the neck radius, was determined from the image. A reference circle is shown for comparison. The radii of the two beads were selected to be within about 10% of one another and were typically on the order of about 1 mm. The sintering times and temperatures where chosen so that the neck diameters could be conveniently measured between 0.02 and 0.1 mm.

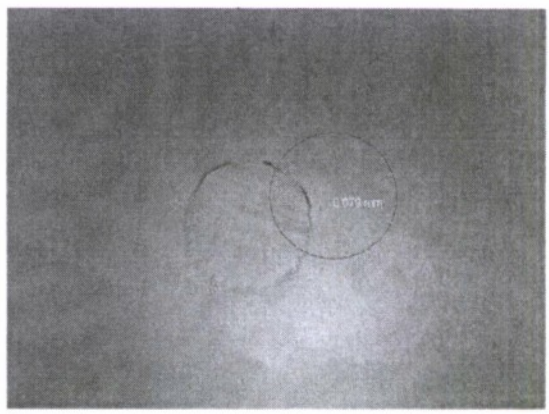

Fig. 2. Optical micrograph of sintering neck between two glass beads as viewed along the common axis. Blue circle and number corresponds to equivalent diameter of neck.

In order to estimate the viscosities from Eq. 1, the surface energies of the glasses were estimated from component contributions to the overall surface energy of oxide melts. The component contributions were combined additively using the procedure outlined by Dietzel and Lyon.[3, 4] In silicate melts, the contributions from oxide components could be classified into three categories according to their partial molar surface energies, γ'. In the first category includes SiO_2, Al_2O_3 and La_2O_3, the partial molar surface

energies are nearly eonstant regardless of their eoneentrations.[5] The partial molar surfaee energies of eomponents like P_2O_5 are eoneentration dependant although their overall eontributions are usually small. Finally, there are other oxide eomponents that have strong eoneentration dependenees and eontribute negatively to the overall surfaee energy. Fortunately, there are none sueh eomponents for our eompositions of interest. Therefore, we estimated the surfaee energies assuming that the eontribution of P_2O_5 to be negligible and aceepting literature values for SiO_2 (3.4×10^{-3} N/m), Al_2O_3 (6.2×10^{-3} N/m), and La_2O_3 (6.4×10^{-3} N/m).[6] The estimated surfaee energies are listed in Table 1 for eompositions ranging between $30Al_6Si_2O_{13}$·$70LaPO_4$ (30M) and $80Al_6Si_2O_{13}$·$20LaPO_4$ (80M).

Table 1. Surfaee energies and estimated viseosities for typieal sintering experiments of $Al_6Si_2O_{13}$-$LaPO_4$ glasses

	Sintering Temperature (°C)	Surfaee Energy (10^{-3} N/m)	Viseosity (Pa·s)	Standard Deviation (Pa.s)
30M	920	486	1.74E+10	4.73E+09
40M	930	495	9.74E+08	4.88E+08
50M	950	503	4.84E+08	1.28E+08
60M	950	510	3.06E+09	1.37E+09
80M	950	523	1.59E+10	3.99E+09

III.A.2. *Viscosities from Densification Measurements of Glass Powder Compacts.* The seeond experimental method for determining viscosities was based on measuring the densities of powder compaets as a funetion of time for different glass eompositions. As with the previous method, evaluation is based on the Frenkel interpretation of viscous sintering, although the data used for evaluation is based more on the statistieal averaging of many partiele eontaets in the within the powder eompaet. To do this, we relied on the method of Seherer.[7]

The apparent density of a pellet, ϱ, was determined from the overall mass of the powder compaet and its external dimensions. Figure 3(left) shows an example of the evolution of relative density with time for a sintered glass pellet of composition $50Al_6Si_3O_{13}$·$50LaPO_4$ (50M50L) and annealed at 950°C. Relative density is the ratio of the apparent density and the true density of the glass ϱ_s as determined by helium displacement pycnometry of the loose powder before sintering.

Raman spectra taken of the glass pellet at different stages indieated that erystallization did not initiate until sometime between 30 and 54 minutes of annealing. The final relative density of 92.8 % was aehieved after almost 1 hour.

Seherer[7] developed a viscous sintering model for powder eompaets based upon Frenkel's assumption. While Scherer's derivation was based on an ideal eubie array of particles that melded into interseeting eylinders, his model has proven applicable for most real packing configurations observed in experiments. The relative density of the pellet is determined by the ratio (x) of its eylindrieal radius (a) and thiekness (l). The model is valid up to ϱ/ϱ_s=0.942, when $x=a/l$ equals 0.5 and all pores are closed. The evolution of x with time is related to a kinetic parameter defined as $K=(\gamma/\eta r_0)(\rho_s/\rho_0)^{1/3}$. The produet of this and the effeetive time of

sintering, $K(t-t_0)$, is referred to as the reduced time. This is determined experimentally from the geometric measurements of the sintered compact whereby

$$K(t-t_0) = \int_0^x \frac{2dx}{(3\pi - 8\sqrt{2}x)^{1/3} x^{2/3}} \tag{2}$$

The subscript "0" represents the value before sintering, and r_0 corresponds to the initial average particle radius before sintering, i.e., 3.5 μm for 50M50L glass powder. By plotting $K(t-t_0)$ as a function of sintering time, K can be determined from the slope.

Figure 3 (right) shows a linear fit between the experimental and reduced times, where an average slope of 1.51 10^{-4} (R = 0.990) was obtained when using all of the data for the first 30 minutes. The slope is greater when using the data for the first 12 minutes, where the slope is 2.07 10^{-4} (R = 0.997). This latter value of K is likely to be a more accurate indicator of the viscosity for reasons related geometrical changes or, possibly, crystal nucleation that was undetected. As such, the viscosity was determined from the experimentally determined value of K and its definition. That is,

$$\eta = \frac{\gamma}{l_0} \cdot \left(\frac{\rho_s}{\rho_0}\right)^{\frac{1}{3}} \cdot \frac{1}{K} \tag{3}$$

Here, the viscosity is inversely proportional to K and assumes that the surface energy is constant during sintering.

At an initial relative density of 0.6, the corresponding x is 0.322, and r_0 is 10.87 μm, the viscosity calculated from Eq. (3) is 3.64 10^8 Pas. The Scherer model assumes that the particle size is uniform and is a characteristic dimensional parameter throughout sintering. This is not likely to be the case since it is expected that some coarsening will take place. This is perhaps one reason

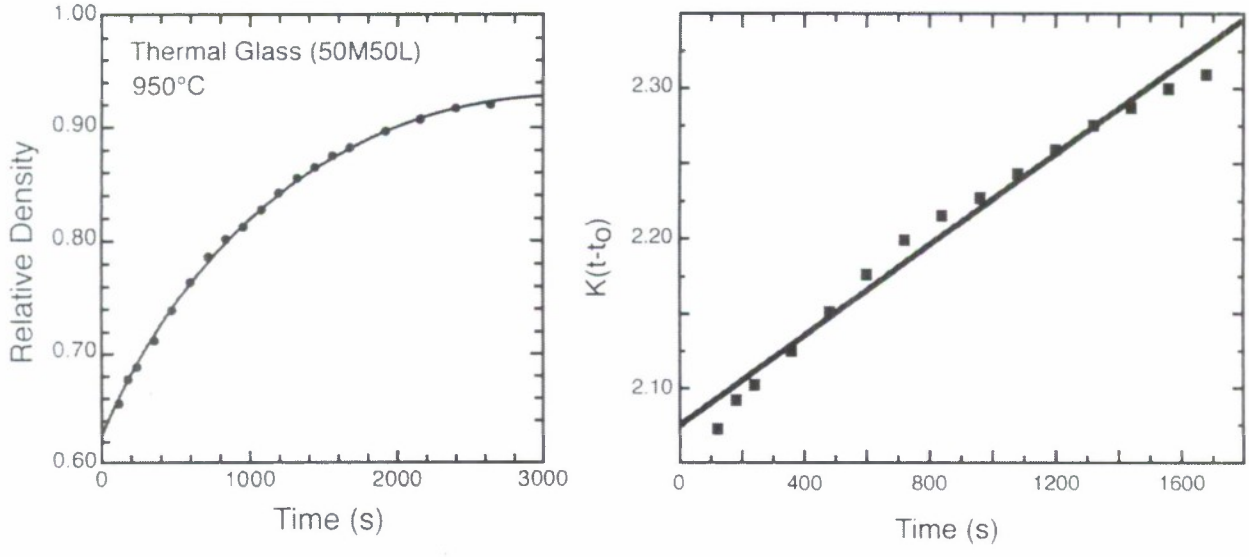

Fig. 3. **Left:** Relative density of glass pellet with time annealed at 950°C. Overall composition is 50/50 mullite ($Al_6Si_2O_{13}$) and lanthanum phosphate ($LaPO_4$). **Right**: Application of Scherer method for analyzing viscosity from sintering data. Plots "reduced" time as a function of actual sintering time.

for the curvature seen in the data. The calculated viscosity is also sensitive to the precision of r_0. Despite this, the calculated viscosities agree well with those from the Frenkel bead experiments ($4.84\ 10^8$ Pa.s), and with viscosities inferred from the DSC thermal analysis (next section) of the glass transition ($1.10\ 10^9$ Pa.s).

Due to partial crystallization, a completely dense glass pellet could not be prepared by pressureless sintering at 950 °C. Lowering the anneal temperature postpones the onset of crystal nucleation, but it will also lower the sintering rate. Optimization is needed to balance these two effects. Reduction of the particle size does help to work around this by accelerating the sintering at a given temperature. We have not yet explored this option. Hot pressing is another alternative that will accelerate sintering. The process can be accelerated by 100 fold when conducted under at 30 MPa hydrostatic pressure. We have demonstrated the capability of producing a translucent glass pellet with the composition of $50Al_6Si_2O_{13}$•$50LaPO_4$ by hot pressing at 925 ° C for 5 minutes under 500 MPa pressure. These results are summarized in section III.B.

III.A.3. *Comparing Viscosities Derived from Sintering and Thermal Measurements*. There have been significant advances in recent years in quantitatively relating the viscosity of inorganic oxide glasses and melts to the details of the thermal signature of the glass transition as determined from and differential scanning calorimeter (DSC). We have applied these observations, with some improvements of our own to the phenomenology, to selected REAPS glasses with very satisfactory agreement.

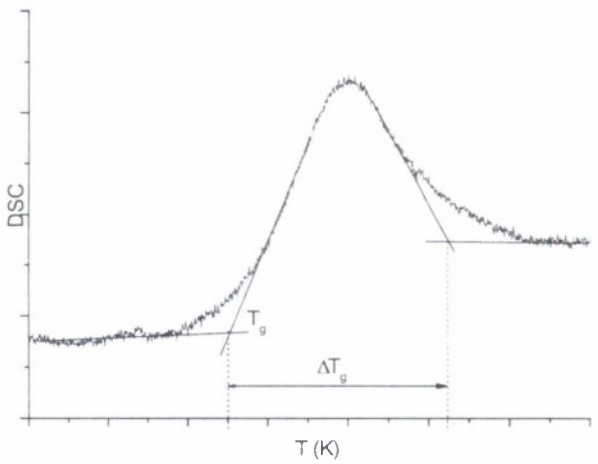

Fig. 4. Example of a DSC thermal trace of a glass transition. The temperature of onset and completion are shown by the intersection of extrapolated lines. The glass transition range is shown as ΔT_g.

The essential quantitative features of the glass transition are the magnitude of the glass transition temperature itself, the width of the glass transition region, and the enthalpic increase due to the glass transitioning into a supercooled liquid. Cooper, Gupta and Moynihan[8, 9] demonstrated that this correlation exists. Their analyses led to the conclusion that the activation for shear viscosity, ΔH^*_η, appropriately characterized the enthalpic contributions. As such, the expression

$$C = (\Delta H^*_\eta/R)(1/T_g - 1/T_g') \qquad (4)$$

was derived, where T_g and T_g' are the temperatures marking the extrapolated onset and the completion of the transition region on a DSC thermal trace, C is a dimensionless constant which is around 4.8 for most high T_g inorganic glasses and R is the gas constant. Figure 4 exhibits an example of a thermal trace of a glass transition and how T_g and T_g'(= T_g + ΔT_g) are determined. The fulfillment of the Eq. (4) requires that the ratio of the quench rate for producing the glass in the first place to the heating rate of the DSC experiment should be between 0.2 and 5 for best

results. In our own case, the quench rate is far faster, although we discovered that comparisons to experiment still remain reasonable.

At temperatures close to T_g, the logarithm of the viscosity, log η, is almost linear with respect to 1/T. It can be deduced that the magnitude of viscosity changes over the glass transition region is about $C/\ln 10 \approx 2.1$ orders of magnitude. This is a useful parameter for developing a relationship between viscosity and the values of T_g and T_g'.

The viscosity of most glasses over certain temperature range can be fit to the empirical Volmer-Fulcher-Tammann (VFT) equation[10-12]. Here,

$$\eta = \eta_\infty \cdot \exp\left(\frac{DT_0}{T - T_0}\right) \tag{5}$$

where η_∞ is a constant and represents the high temperature viscosity limit, D and T_0 are constants that relate to what is now described as a glass's fragility. (Fragility is in essence a measure of the deviation of a glass's viscosity from Arrhennian behavior.)

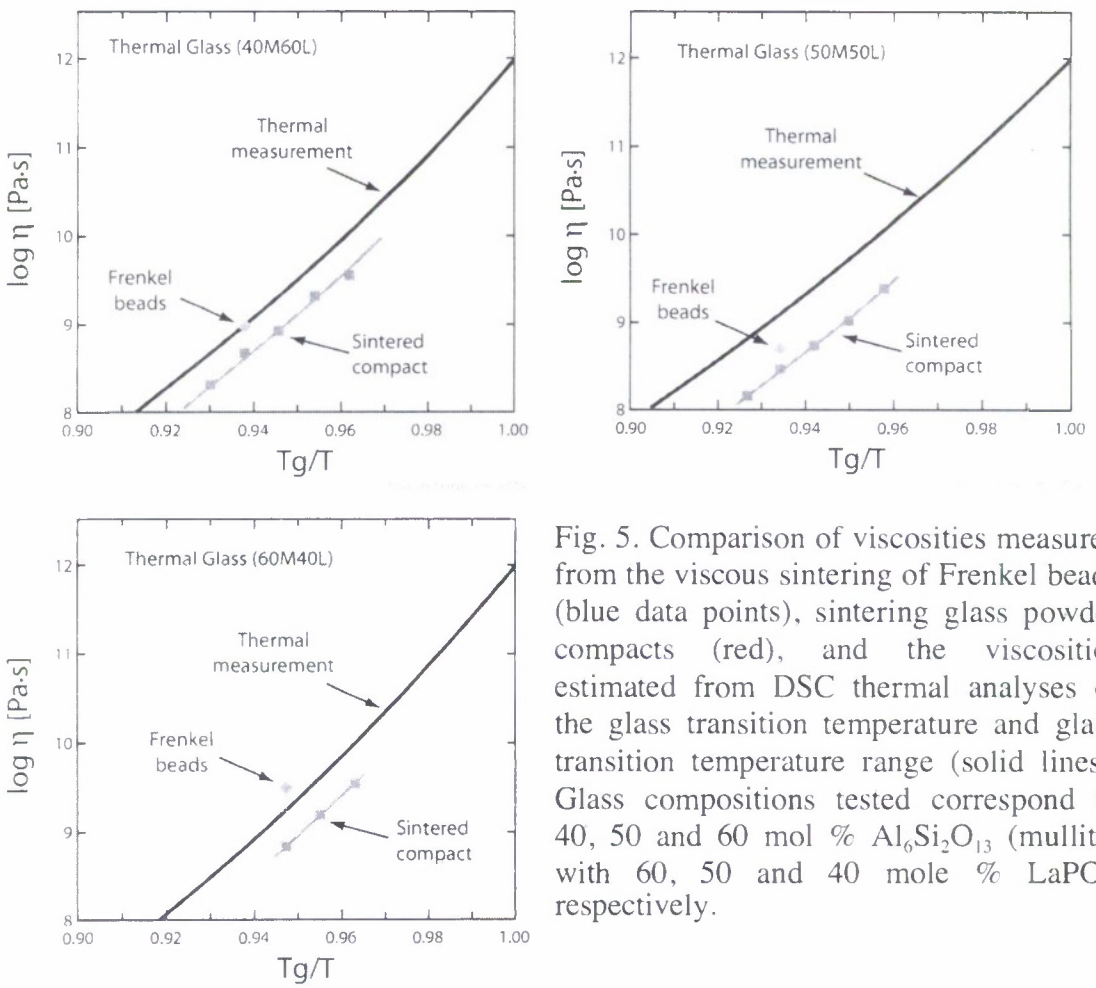

Fig. 5. Comparison of viscosities measured from the viscous sintering of Frenkel beads (blue data points), sintering glass powder compacts (red), and the viscosities estimated from DSC thermal analyses of the glass transition temperature and glass transition temperature range (solid lines). Glass compositions tested correspond to 40, 50 and 60 mol % $Al_6Si_2O_{13}$ (mullite) with 60, 50 and 40 mole % $LaPO_4$, respectively.

Based upon these equations, and the various parametric and quantitative aspects of a glass transition thermal behavior, we were able to derive equations for predicting the viscosity of our REAPS glasses to the relatively simple equation of

$$\log\eta = (-17 + \log\eta_{T_g}) + \frac{120.6 \cdot \Delta T_g}{(T - T_g + 6.62 \cdot \Delta T_g)} \qquad (6)$$

Here, ΔT_g is the width of the glass transition region and η_{Tg} is the viscosity at the onset of glass transition. For most glasses, the viscosity at the glass transition temperature is 10^{12} Pa•s and which is assumed in this study. Equation (6) suggests then that the viscosity of a glass and supercooled liquid above the glass transition temperature can be predicted by measuring T_g and ΔT_g in a single DSC experiment.

To test this equation, Fig. 5 compares the experimentally determined viscosities for several compositions from the sintering studies with those predicted by Eq. (6) using the thermal analysis studies. There is generally good agreement between all data sets, although the DSC estimated values tend to be greater than either of the two sintering experimental approaches. The difference can be attributed to the deviation of the powder experiments from the ideal assumptions of Scherer's model used to interpret the results. Nonuniform particle sizes, and nonideal powder packing are two important considerations.

Overall, it appears that viscosities inferred from the DSC thermal analyses are quite reliable. In fact, there is sufficient uncertainty in the interpretation of the sintering studies that one might assume that the DSC-based determinations are perhaps more accurate. With a more sophisticated analysis of the sintering studies, it is expected that the data points would more closely match the DSC measurements. The agreement of the slopes in Fig. 5 is very striking for all three compositions. This increases our confidence in using estimated viscosities derived from the glass transition temperature measurements.

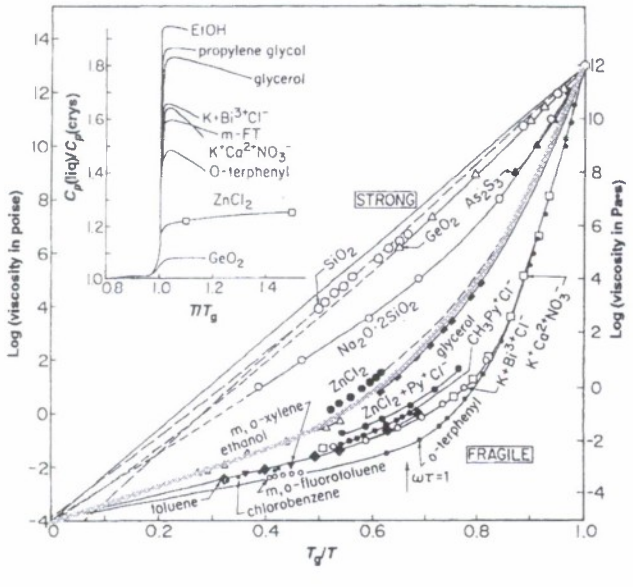

C. A. Angell, Science, 267, 1924-1935 (1995)

Fig. 6. Comparison of typical viscosities of REAPS glasses to the full range of glasses in context of an Angell plot[1].

Putting this into context of all glasses, Fig. 6 compares the typical viscosities of REAPS glasses with respect to the full range of observed glasses. This plot is in the format of an Angell fragility plot[1]. As far as inorganic glasses are concerned, REAPS glasses deviate significantly from the linear behavior typical of Arrhennian behavior of many activated processes. As such, REAPS glasses are considered to be quite "fragile" as compared to "strong" glasses like SiO_2. This may be interpreted to large degree of structural changes in the glass

network with temperature near the glass transition. This attests to the complexity of the glass structure due in part to the network formed from three different tetrahedral species. It should also be noted that in the range of about 100-200°C above the glass transition temperature, these glasses often exhibit amorphous phase segregation while in the supercooled liquid state. As described in our earlier report, this precedes a complex sequence of processes that lead to the nucleation and growth of composite structures of mullite and lanthanum phosphate monazite.

III.B. Comparing Sol-Gel Derived and Thermally Quenched Glasses.

We undertook a preliminary study to test two different chemical routes toward producing REAPS glasses by sol gel synthesis and compared them to our standard process of quenched-melt synthesis. One motivation was to search for low temperature routes that produced a greater quantity of glass than is typical from our current set up for melting and quenching. This latter method typically produced on the order of a gram to a few grams of glass in a typical run. On the other hand, we were interested in developing methods for producing tens or hundreds of grams of material that possessed the characteristics that were most critical for extended studies on nucleation-growth-microstructural control studies for ceramic-matrix-composites. Those characteristics included exhibiting the same glass transition temperatures as for thermal glasses and were capable of being densified without significant crystallization. One of our chemical routes is very promising for this purpose. However, the other chemical route introduces another concept of producing dense composites of highly porous, but mechanically rigid, composite foams. This section focuses on the sol gel chemistries we tested and compares their general properties to the thermally derived glasses. Succinctly, there are similarities in glass transition behavior and other glass properties, but there are also distinct differences in their crystallization behavior. There are clear advantages seen in using both types of glasses for composite fabrication. It is intriguing to us that hot pressed billets from thermal glasses produced dense and transparent glass, whereas billets from sol gel glasses produced dense and transparent crystalline composites of very fine microstructures. We see promise in both materials.

III.B.1 Preparation of $50Al_6Si_2O_{13}$-$50LaPO_4$ Xerogels

The preparation of the $Al_6Si_2O_{13}$-$LaPO_4$ glass by melt quench method has been reported, and the glass has to be melted over 2000 °C due to the high liquidus temperature. $LaPO_4$ decomposes partially at such a high temperature with release of phosphorus oxides, and the glass is phosphorus deficient. Sol-gel technique has been used to prepare glass at the temperature much lower than the melting point of glass. The preparation of mullite via sol-gel techniques has received attention for more than 20 years[13-15]. During this time, the different gel types have been distinguished by the degree of their homogeneity of mixing between Si and Al. A single phase gel refers to molecular level mixing, whereas a diphasic gel will consist of Al-O clusters at ~5 nm level or greater[16, 17]. The preparation of gels for the $Al_6Si_2O_{13}$-$LaPO_4$ system has not been reported. The possibilities of preparing bulk $Al_6Si_2O_{13}$-$LaPO_4$ glass from the xerogel by viscous sintering is investigated here. The $Al_6Si_2O_{13}$-$LaPO_4$ gels based on both single phase and diphasic mullite gels have been prepared from tetraethoxysilane (TEOS) and aluminum isopropoxide or aluminum sec-butoxide.

III.B.1.1. Preparation Procedures

III.B.1.1.1. $Al_6Si_2O_{13}$-$LaPO_4$ gels based on single phase mullite gel. Homogeneity of the single phase gel is at the molecular level. Mullite crystallizes at low temperatures, e.g. 1000°C, and no spinel phase appears. Aluminum isopropoxide was dispersed in 100% ethyl alcohol (C_2H_5OH) at an Al:C_2H_5OH molar ratio of 1:15 by vigorous stirring, and white viscous suspension was obtained after 24 hours. TEOS was added to the viscous suspension with a Al:Si molar ratio of 3:1, i.c. the Al:Si molar ratio in mullite, followed by adding 2M HNO_3 with a Al:H^+ molar ratio of 1:0.5. After adding TEOS, the suspension became more viscous and formed gel almost immediately, and the gel dissolved gradually after adding of HNO_3. After 4-6 hours rigorous stirring, a sol as clear as water was obtained. The sol was cast into a covered plastic dish for gelling and drying to prepare mullite gel. La and P were introduced into sol by $La(NO)_3.6H_2O$ and trimethylphosphate (TMP) to prepare the gel with 50 mol% concentration (50M). The sol was still clear after the introduction of La and P and was stirred for further 4 hours and cast. The sol formed gel within 7 days with a large amount of solvent evaporation.

III.B.1.1.2 $Al_6Si_2O_{13}$-$LaPO_4$ gel based on diphasic mullite gel. The homogencity of the diphasic mullite gel is in ~10 nanometer level, and spinel forms during at about 1000 °C and transforms to mullite at about 1280 °C. Aluminum isopropoxide hydrolyzed in H_2O at an Al:H_2O molar ratio of 1:25 for 6 hours or longer, and a white suspension formed. 2M HNO_3 (H^+:Al=0.5) were added, and the sol became very viscous and translucent after 1 hour stirring. Unhydrolyzed or prehydrolyzed TEOS, $La(NO_3).6H_2O$ and TMP were added sequentially every 1 hour with vigorous stirring to prepare 50M gel. Translucent pure mullite gel and the $Al_6Si_2O_{13}$-$LaPO_4$ gels were cast into the covered disk for further use.

III.B.1.1.3. $Al_6Si_2O_{13}$-$LaPO_4$ gel with homogeneity between the single phase and diphasic gel. Starting from aluminum sec-butoxide, water (H_2O:Al molar ratio = 1:25) and 2M HNO_3 (Al:H^+ molar ratio=1:0.5) was added and a white suspension formed with the release of heat. After vigorous stirring for 24 hours, a clear solution formed that subsequently separated into two solutions. The top layer was composed of sec-butanol, which dissolves almost no water. This was cvaporated away leaving behind the lower layer consisting mostly of the hydrolyzed aluminum sol.

Next, aluminum isopropoxide was mixed with H_2O at an Al:H_2O molar ratio of 1:25 for 4 hours or less, and 2M HNO_3 (H^+:Al=0.5) were introduced. After 24 hours, a translucent and non-viscous sol forms.

La and P werc introduced as described above. Un-hydrolyzed TEOS or pre-hydrolyzed TEOS (TEOS: C_2H_5OH:H_2O: HNO_3=1:4:10:0.04) were added to the prehydrolyzed aluminum alkoxide solution. The mixture was stirred until clear and cast. The sol with unhydrolyzed TEOS forms gel in about 1 week. The sol with prehydrolyzed TEOS forms gel in 5 minutes after adding TEOS, and the gel forms clear sol again in 1 week, then the final gel forms in another 1 week.

Since this gel behaves like the single-phase gel except that it shows a small amount of spinel and a weak pcak corresponding to the spinel-mullite transformation, *semi single phase* gel is used to denote this kind gel.

III.B.1.1.4 Preparation of xerogels. The air dried single phase gels were dried further at 60 °C for 1 day and 120 °C for 1 day, heated to 800 °C at 1 °C/min and sintered for 4 hours. The air

dried diphasic gels were dried at 80°C for 4 hours, heated to 650 °C at 1 °C/min and sintered for 5 hours.

III.B.1.1.5 Pressureless sintering. The xerogels were ground and particle sizes below 35 μm were separated out. Pellets were made by pressing powder under a uniaxial pressure of 400 MPa. The sintering was finished in a preheated tubing furnace under air atmosphere. All the samples are quenched after each sintering.

III.B.1.1.6 Hot pressing. The gel and thermal glass powders were each ground and sieved to pass through a No 400 mesh screen as starting materials. The sieved powder, i.e. under 35 μm, was loaded into a platinum capsule and sintered in a carbon furnace under a semi-isostatic pressure of 500 MPa. The temperature was controlled through a thermal couple attached to the platinum capsule. The capsule was heated at a rate of 20 °C/min and quenched after sintering. The pressure was maintained at 500 MPa for the whole sintering process.

III.B.2 Characterization of Xerogels

III.B.2.1 Xerogel appearance. After calcinations, the single phase and the semi single-phase 50M gel were composed of clear particles around ~10 μm, while the diphasic 50M gel consisted of translucent particles 1-5 mm in size. The densities of both gels were measured by helium displacement pycnometer after annealing and degassing at 600°C for 30 minutes. The density of the diphasic 50M xerogel had a similar density as thermal quenched glass of 3.2 g/cm^3, while that of the single phase 50M gel was 2.7 g/cm^3. 20 hours after degassing, the densities of the gels were measured again. It was found that the density of diphasic gel decreases about 7% and that of the single phase gel showed a slight decrease no more than 1%. The difference of the homogeneous level of the single phase and the diaphasic gel might explain the different behavior of density change with time. The homogeneous level of single phase 50M gel was similar to cluster size of the acid catalyzed silica gels prepared from silicon alkoxides, which shows a lower porosity and a lower skeletal density, while the homogeneous level of diphasic gel is similar to the cluster size of base catalyzed silica gels or particulate gels, which has a higher porosity and a higher skeletal density[16]. The measured densities and the density of thermal glass are shown in Table 2.

Table 2 Density of 50M thermal glasses and gels

	Density after 600 °C degassing (cm^3)	Density after stayed in air for 20 hours (g/cm^3)
Thermal quench 50M glass	3.22	3.22
Single phase 50M gel	2.59	2.57
Diphasic phase 50M gel	3.26	3.04

III.B.2.2. XRD results of the xerogels and fully crystallized sample

Both the single phase and diphasic xerogels are amorphous under X-ray diffraction, as shown in Fig. 7, and the positions of the wide humps in the pattern are close to that of the thermal quench glass except a wide peak centered at $2\theta=67°$ in the pattern of the diphasic gel. The peak can be assigned to the disordered Al-Si spinel, which grows stronger and sharper with the heating temperature and time.

All the gels and glasses are fully crystallinc after a 1400 °C as shown by XRD Fig. 8. Abovc the crystallization temperature, only Al-Si spinel, mullite, orthorhombic and monoclinic $LaPO_4$ phases are observed. The fully crystalline single phase gel shows the phases of mullite, orthorhombic and monoclinic $LaPO_4$, and the fully crystalline diphasic gel is composed of mullite and mono clinic $LaPO_4$ only. The XRD pattern of the 50M thermal glass shows a higher concentration of orthorhombic $LaPO_4$ and an additional $LaAl_{11}O18$ pattern except those of mullite and $LaPO_4$. The ratio of the monolithic and orthorhombic $LaPO_4$ may relate with the homogeneity of the mixture. Since the sequence of the homogeneity level is the thermal glass, the single phasc gel and the diphasic gel. The appearance of the $LaAl_{11}O_{18}$ phase is due to the phosphorous loss during the high temperature melting as proven by the composition analysis of the thermal glass.

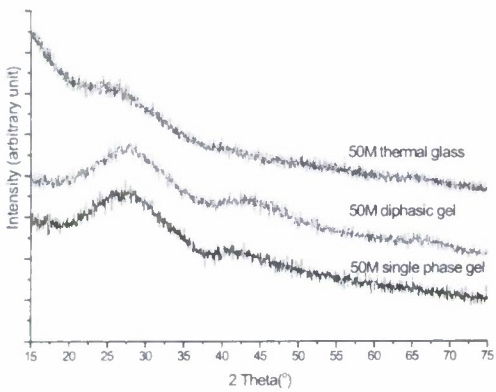

Figure 7 The XRD patterns of the 50M thermal glass, calcined diphasic and single phase xerogels

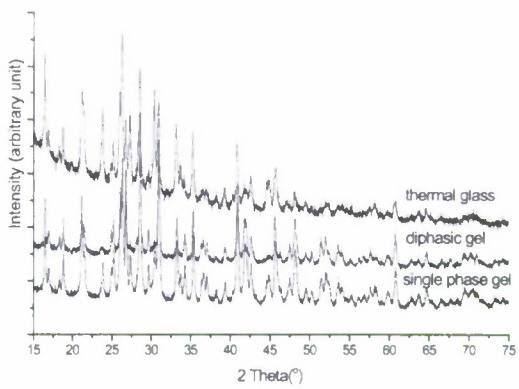

Figure 8 The XRD patterns of the thermal glass, single phase gel and diphasic gel after heated to 1400°C

III.B.2.3. DSC thermal analysis of the xerogels

The DSC thermal signatures for both mullite single phase and diphasic gels are shown in Fig. 9. The single phase gel shows two strong exothermic peaks at about 950 °C and 1000 °C. These correspond to the formation of orthorhombic mullite. The diphasic gel shows only onc peak at about 1280 °C, and it has been found that an aluminosilicate spinel forms in the diphasic gel, which then transforms to mullite at about 1280°C[18]. The DSC trace of the semi single-phase gel shows a weak 1280°C peak on top of what is the normal single phase thermal signature.

Combined DSC/TG traces of the gels are compared to that of the thermal glass in Fig 10. As expected, the thermal glass exhibits no weight loss up to 1400°C and only a weak and broad exothermic DSC peak between 200-1000°C that is attributed to structural relaxation. The glass transition occurs at 879 °C, and simultaneous crystallization of the orthorhombic $LaPO_4$ and $Al_6Si_2O_{13}$ occurs at 1063 °C. The exothermic peak at 1245°C may correspond to the phase transformation $LaPO_4$ from the orthorhombic and monoclinic $LaPO_4$ or the spinel to mullite. Please note that although no spinel phase appears in the whole thermal process of the single phase, mullitc gel, it does appears in the single phase mullite-$LaPO_4$ gcl.

The single phase gel shows little weight loss just below the first exothermic peak, and behaves much like a thermal glass. The broad exothermal peak may also be mainly due to the structure

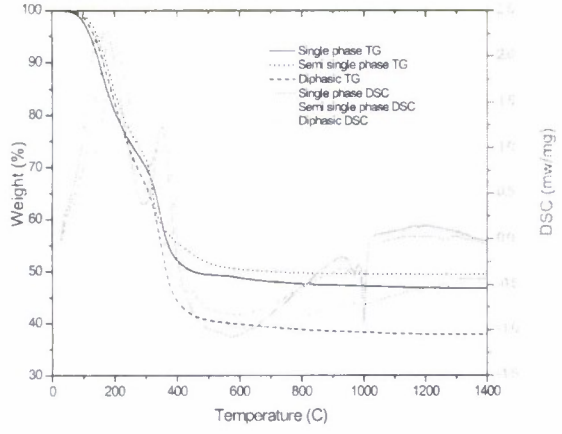

Figure 9. DSC and TG curve of the single phase, semi single phase and diaphasic gels

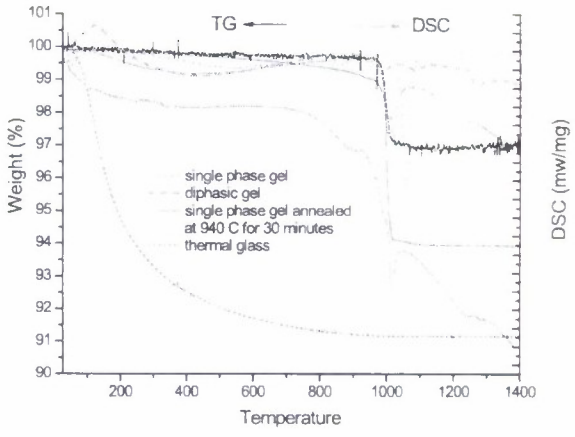

Figure 10. DSC and TG curves of the thermal glass, single phase xerogel, diphasic xerogel and single phase gel with an additional annealing at 940 °C for 30 minutes.

relaxation. The small endothermic peak centered at 930 °C repeats with the same position and area as the 3 cooling and heating cycles up to 950 °C was done, so it is assigned to the glass transition and the onset of the glass transition temperature is at 920 °C. The sharp exothermic peak at 1004 °C accompanied by the almost instant weight loss is the most obvious park of the DSC curve. Heat the gel at 20 °C/min to 985 °C, i.e., higher than the onset of this exothermic peak, and then quench, and the gel is still amorphous under XRD, so the exothermal peak is caused by the weight loss solely. DSC curve of the single phase gel with an additional annealing at 940 °C for 30 minutes retain all the thermal signatures of the unannealed gel except the weaker first exothermic peak and less weight loss.

The assignment of this thermal signature is discussed in detail in the following chapter coupled with Raman and FTIR results. Through the CHN element analysis of these gels, it has been found the weight loss is due to the burning of carbon and nitrogen. As shown in Table 3, the 800 °C as calcined single phase gel has about 0.6 wt% carbon and 1.8 wt% nitrogen. At 925 °C , a slow burn out of carbon and nitrogen is observed, while their concentrations decrease sharply with the annealing at 950 °C or higher. Annealing the gel at 950 °C for 30 minutes burns out almost all carbon and nitrogen. The TG curve of the diaphasic shows a steep weight loss at 100-200 °C, corresponding to an endothermic peak centered at 124 °C in the DSC curve, and this is caused by the loss of the absorbed free water. A gradual weight loss up to 1000 °C in the TG curve and the broad exothermic peak at 200-1000 °C in the DSC curve is due to the combined effect of condensations and structure relaxations. The first exothermic peak at 995 °C corresponds to the crystallization of spinel, and the second exothermic peak at 1088 °C corresponds to the crystallization of orthorhombic $LaPO_4$. The exothermic peaks at 1272 °C correspond to the phase transformations of spinel and $LaPO_4$. Diphasic gel has no carbon and nitrogen residue, but it has a hydrogen concentration of 0.57 wt%. It may be attributed to the residue hydroxyls and the absorbed water in its pores.

Table 3. The carbon, nitrogen and hydrogen concentration of single phase gel at difference annealing conditions

	Carbon (wt%)	Hydrogen (wt%)	Nitrogen (%)
As calcined	0.575	0.006	1.821
925 C for 4 hours	0.119	-0.058	0.442
950 C for 10 minutes	0.353	-0.072	1.143
950 C for 30 minutes	0.06	-0.074	0.243
950 C for 4 hours	0.051	-0.05	0.149
1200 C for 60 minutes	0.074	-0.048	0.13

III.B.2.4. Raman and IR spectra of the xerogels

As shown in Fig. 11, the Raman spectra of the single phase xerogels exhibit several broad vibrational bands between 100 and1200 cm^{-1}. Compared with the Raman spectrum of the thermal glass, the center of the intense and broad band between 800 and 1200 cm^{-1} shifted from ~1010 cm^{-1} to ~1060 cm^{-1}, and it exhibits additional sharp bands at 1285, 1388, 1558 cm^{-3}. For the single phase gel annealed at 925 °C for 4hr, the decrease of the intensity of these three peaks, as well as the weight loss in the TG curve and the accompanied sharp exothermic peak in the DSC curve was observed. The single phase gel shows little weight loss after firing at 950 °C for 30 minutes, and the three sharp peaks also almost disappear in the Raman spectrum. Therefore, these three peaks must relate to the structural and composition change caused by the weight loss. The broad Raman bands indicate the general disorder of the structure as that of the thermal glass. The intense and broad 800-1200 cm^{-1} band are assigned to the stretching vibrations of PO_4 unit, and the less intense bands between 350-450 cm^{-1} and 550-650 cm^{-1} are related to the bending vibrations of O-P-O bonding. The Raman spectrum of the diaphasic gel exhibits similar bands position and relative intensity as the thermal glass. The Raman spectrum of fully crystallized 50M gel is almost identical to that of the crystalline $LaPO_4$.The FTIR spectra of the gels and thermal glass are shown in Fig. 12. The as-calcined amorphous gel shows almost no characters below 1200 cm^{-1}. The diphasic gel exhibits strong OH vibration at about 3400 cm^{-1} and 1600 cm^{-1}, which can be assigned to the absorbed water and the residual hydroxyls. The single phase gel exhibits much weaker OH vibration bands, but with a intense and sharp bands at 2345 cm^{-1}, and three weak and sharp bands at 2777, 3599 and 3705 cm^{-1}. The four bands may have the same origins as the three sharp peaks in the Raman spectra because they also fade with the heating time and temperature as shown in the spectra of the single phase gel annealed at 925 °C for 4 hours and 950 °C for 30 minutes. With the weight loss at high temperature, the single phase gel swells and creates pores which provide sites for absorbing water, and the IR spectra of the annealed gels exhibit stronger OH vibrations than the as calcined xerogel.

III.B.3 Pressureless sintering of the single phase gel

We carried a series of sintering experiments of single phase xerogel derived, glass powders under atmospheric conditions. The results were not typical of the viscous sintering behavior seen for thermal glasses (described in an earlier report) because of considerable foaming. More normal behavior was seen for the diphasic gels, presumably because of the much reduced organics used in the process. What is interesting about the foaming behavior of these materials

was the ability to form composite structures of relatively low densities and which remain microstructurally stable to high temperatures. As mullite-monazite composites, this suggests that it will be possible to produce low-density, open framework ceramics of high fracture toughness. This would be appealing for applications requiring both thermal resistance and mechanical stability.

Figure 13 presents a collage micrographs of the foam structures observed for different sintering and annealing conditions. Figure 13a is that of single phase xerogel sintered at 925°C. Sintering was followed by helium pycnometry of samples interrupted at different stages of the process. We also followed the crystallization behavior by high temperature x-ray diffraction (not shown), which was correlated with the thermal analyses. The microstructure shown corresponds to a sample consisting of 84% open porosity and 3-4% closed porosity. (This infers a bulk density of 10 to 12% of theoretical.) The pore size distribution is clearly bimodal. The large pores are typically open and interconnected. However, the glass walls between these large pores consist of pores that are much smaller and closed. The picture that emerges is that viscous sintering occurs at early stages at lower temperatures as the sample is heated. Subsequent to this, foaming begins as residual organics react and reduce phosphorous, which then expands due to its high vapor pressure. Subsequent to this, the larger pores break open to the atmosphere and either re-oxidize or sublime away.

The other micrographs in Fig. 13 correspond to subsequent anneals at higher temperatures and

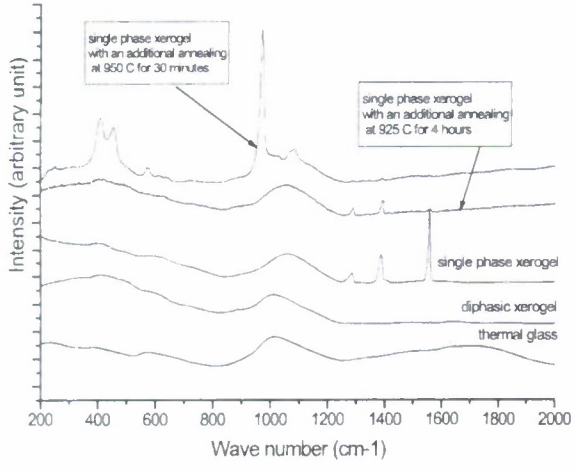

Fig. 11. Raman spectra of single phase and diphasic xerogels, thermal glass and a preannealed single phase xerogel.

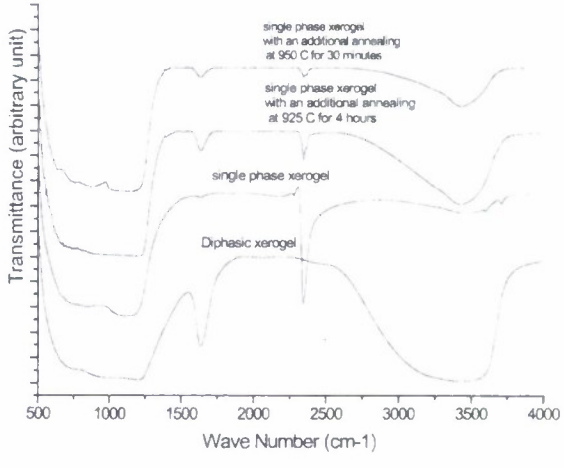

Fig. 12. Transmittance IR spectra of the diphasic gel, the as calcined single phase xerogel and the single phase gels with additional annealings

longer times to illustrate the stability of the porous microstructure. The conditions range from the sintering conditions at 950°C over minutes to 1400°C over several days. The microstructure after annealing at 1200°C and 60 minutes remained stable, which in fact exhibited slightly lower densities and greater open porosity. At this point, the glass has completely converted to crystalline mullite and monazite. Although we have not examined directly the crystalline composite structure in the network walls of this foam, the size features are clearly going to be small considering that the wall thicknesses between the large open cells are in the range of 100 to

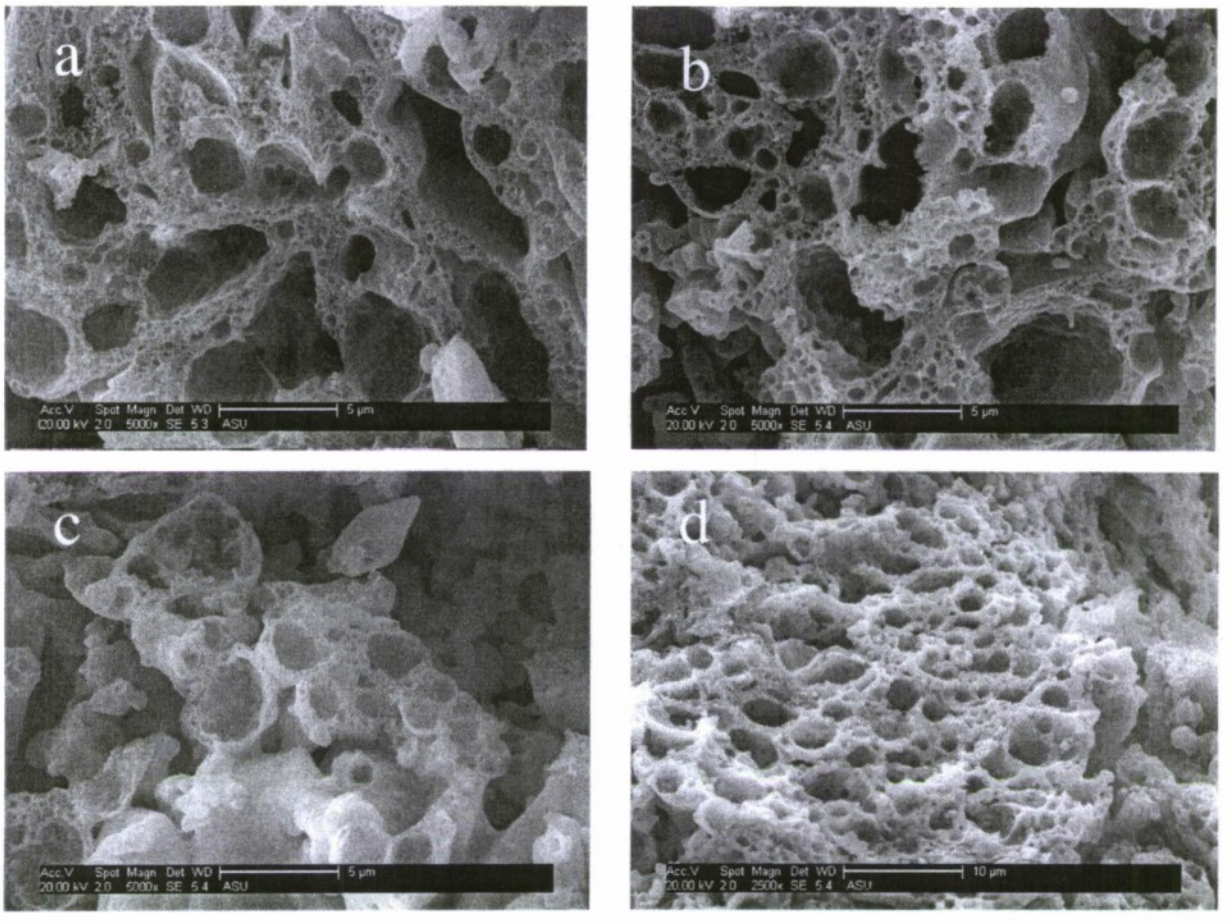

Figure 13 SEM pictures of the single phase xerogel sintered at (a) 950 °C for 10 minutes, (b) 950 °C for 30 minutes, (c) 1200 °C for 60 minutes, and (d) 1400 °C for 7 days.

200 nm. The microstructure after annealing at 1400°C and seven days exhibits some densification although the open porosity still remains at about 70%.

This resistance to densification is attributed to slow the diffusion and coarsening kinetics of the crystalline material. This is as opposed to the glass where viscous flow is much faster at even lower temperatures. These observations affirm the utility of working with glass precursors to form what will be the overall structure of a ceramic composite at low temperatures, which is then crystallized into the composite at higher temperatures. Once crystallized, another protocol controlling relaxation kinetics takes over which offers the advantage of structural stability at higher temperatures.

III.B.4 Hot Pressing: A comparison between thermal and sol gel derived glasses

A comparison was conducted on the ability densify thermal and gel derived powders by hot pressing at temperatures slightly above the glass transition temperature. The emphasis here was to combine pressure with the speed offered by viscous sintering. The thermal glass and the glass from diaphasic gel were hot pressed at 925°C, 30 MPa and 5 minutes. The glass from the single-phase gel was hot pressed at 950°C and 5 minutes.

Figure 14 presents three different cases, comparing the Raman spectra of the powders prior to hot pressing and then densified billet. In two cases, photographs are presented that illustrate the translucency of the samples. In the third case, the hot pressed sample was translucent, although it is not shown here.

The Raman spectrum for the hot pressed thermal glass is shown in the upper left portion of Fig. 14. There is essentially no difference before and after sintering. There is no sharpening of any features and a lack of sharply defined peaks. Evidently, the sample remained amorphous throughout densification. The broad peak centered on about 1050 cm^{-1} corresponds to the bonding stretches within tetrahedrally coordinated phosphorous. The inset photograph shows a translucent, almost transparent, piece of dense glass. Because Raman and X-ray diffraction revealed no crystalline material, and because the pressures were sufficiently high to collapse any gas filled pores, it is assumed that the lack of complete transparency is due to compositional and density inhomogeneities. Our previous studies revealed amorphous phase segregation to occur in thermal annealing glasses between the glass transition and crystallization temperatures at ambient pressures. This suggests that the same is true for this hot pressed sample.

The Raman spectra for the powder and hot pressed sample from powders of single phase xerogels are shown in the upper right portion of Fig. 14. In the powder, the same broad peak appears at 1050 cm^{-1} as for the thermal glass. However, there are sharp peaks at higher wavenumbers. These may be indicative of the presence of retained carbon and nitrogen. This needs to be investigated more before a definitive statement could be made. Crystallization clearly occurred during hot pressing. The peaks near 1000 cm^{-1} indicate the organization of phosphate groups; and the sharp peaks at lower Raman shifts can be attributed to the aluminosilicate components. The peaks at higher wavenumbers indicate the further retention of carbon and nitrogen.

The Raman spectra for the powder and hot pressed sample of the diphasic xerogel preparation are shown in the lower left corner of Fig. 14. Whereas the powder starts off as being amorphous like the thermally prepared glasses, crystallization is clearly shown due to the hot pressing. These spectra are much simpler than for the case of the single phase gel, and even for the case of the thermal glasses. The inset photograph also indicates that the sample is translucent. It is likely that the lack of complete transparency is due to light scattering off of crystallites. Otherwise the appearance and densification of this material is very similar to that of the thermal glass.

Project Participants

Personnel Supported by Grant

Feng He	Graduate Assistant, School of Materials, Arizona State University, Tempe, AZ
Shuling Guo	Post doctoral research associate, Arizona State University, Tempe, AZ
William T. Petuskey	PI, Professor & Chair, Chemistry and Biochemistry, and Professor, School of Materials, Arizona State University, Tempe, AZ

Collaborator

Paul F. McMillan	Professor, Chemistry, University College of London, United Kingdom

Project Activities: List of Presentations

Publication

R. Marzke, S. Boucher, G. Wolf, J. Piwowarczyk, W. Petuskey, "Lanthanum phosphate calcium aluminate glasses: 27Al and 31P NMR spectroscopy," *J. European Ceramic Society*, 28, 2421-2431(2008).

Oral Presentations:

Robert F. Marzke, George H. Wolf, Susan Boucher, Jeremy Piwowarczyk, William T. Petuskey, "Locations of metal ions in the new glasses in the calcium aluminate-monazite system, studied by NMR of ^{27}Al and ^{31}P and by Raman scattering," American Physical Society Annual Meeting, Denver, Colorado, March 5-9, 2007.

W. T. Petuskey, "REAPS Glasses and Glass-Ceramics," Naming Ceremony of the LeRoy Eyring Center for Solid State Sciences (at Arizona State University), Tempe, Arizona, March 2007

W. T. Petuskey, "Complex Glasses as Precursors for Nanocomposites," a conference on materials chemistry entitled *MC8: Advancing Materials by Design*, London, U.K., July 1-4, 2007 (invited).

W. T. Petuskey, Feng He, Shuling Guo and P. F. McMillan, "REAPS to CMC's: The Chemistry and Crystallization of Rare Earth AluminoPhosphoSilicate Glasses, " conference entitled *Composites at Lake Louise*, Lake Louise, Canada; October 28 to November 2, 2007 (invited).

W. T. Petuskey and P. F. McMillan, "REAPS Glasses as Low-Temperature Precursors for High Temperature Ceramics," *International Yoshimura Symposium on Soft Processing*, Komaba Eminence, Tokyo, Japan, March 8, 2008 (invited).

W. T. Petuskey, "Complex Glasses as Low-Temperature Precursors for High Temperature Ceramic *nano*-Composites," *Functional Oxides*, Royal Society of Chemistry spring Solid State Group meeting, University College of London, London United Kingdom, April 14-16, 2008 (invited).

References

1. Angell, C.A., *Formation of glasses from liquids and biopolymers*. Science (Washington, D. C.), 1995. **267**(5206): p. 1924-35.
2. Frenkel, J., *Viscous Flow of Crystalline Bodies Under the Action of Surface Tension*. Journal of Physics (Moscow), 1945. **9**(5): p. 385-391.
3. Dietzel, A., *Practical importance and calculation of the surface tension in glasses, glazes and enamels*. Sprechsaal, 1942. **75**: p. 82.
4. Lyon, K.C., *Calculation of surface tension of glasses*. J. Am. Ceram. Soc., 1944. **27**: p. 186-9.
5. Appen, A.A., *Attempt to classify components according to their effect on the surface tension of silicate melts*. Zh. Fiz. Khim., 1952. **26**: p. 1399-1404.
6. Shimizu, F., et al., *Viscosity and surface tension measurements of RE2O3-MgO-SiO2 (RE = Y, Gd, Nd and La) melts*. ISIJ Int., 2006. **46**(3): p. 388-393.
7. Scherer, G.W., *Sintering of low-density glasses: I. Theory*. J. Am. Ceram. Soc., 1977. **60**(5-6): p. 236-9.
8. Cooper, A.R., Jr. and P.K. Gupta, *A dimensionless parameter to characterize the glass transition*. Phys. Chem. Glasses, 1982. **23**(1): p. 44-5.
9. Moynihan, C.T., *Correlation between the width of the glass transition region and the temperature dependence of the viscosity of high-Tg glasses*. J. Am. Ceram. Soc., 1993. **76**(5): p. 1081-7.
10. Fulcher, G.S., *Analysis of recent measurements of the viscosity of glasses*. J. Am. Ceram. Soc., 1925. **8**: p. 339-55.
11. Tamman, G. and W. Hesse, *The dependence of viscosity upon the temperature of supercooled liquids*. Z. Anorg. Allg. Chem., 1926. **156**: p. 245-57.
12. Vogel, H., *The law of the relation between the viscosity of liquids and the temperature*. Physik. Z., 1921. **22**: p. 645-6.
13. Okada, K. and N. Otsuka, *Characterization of the spinel phase from SiO2-Al2O3 xerogels and the formation process of mullite*. J. Am. Ceram. Soc., 1986. **69**(9): p. 652-6.
14. Pask, J.A., et al., *Effect of sol-gel mixing on mullite microstructure and phase equilibria in the alpha -alumina-silica system*. J. Am. Ceram. Soc., 1987. **70**(10): p. 704-7.
15. Yoldas, B.E. and D.P. Partlow, *Formation of mullite and other alumina-based ceramics via hydrolytic polycondensation of alkoxides and resultant ultra- and microstructural effects*. J. Mater. Sci., 1988. **23**(5): p. 1895-900.
16. Brinker, C.J. and G.W. Scherer, *Sol-gel science: the physics and chemistry of sol-gel processing*. 1990, San Diego: Academic Press.
17. James, P.F., *The gel to glass transition: chemical and microstructural evolution*. J. Non-Cryst. Solids, 1988. **100**(1-3): p. 93-114.
18. Hoffman, D.W., R. Roy, and S. Komarneni, *Diphasic xerogels, a new class of materials: phases in the system alumina-silica*. J. Am. Ceram. Soc., 1984. **67**(7): p. 468-71.